

# Parameters' Identification of Perzyna and Chaboche Viscoplastic Models for Aluminum Alloy at Temperature of 120°C

Paweł KŁOSOWSKI, Anna MLECZEK

*Gdańsk University of Technology, Faculty of Civil and Environmental Engineering  
Department of Structural Mechanics and Bridge Structures*

Narutowicza 11/12, 80–233 Gdańsk, Poland  
e-mail: {klosow, annmlecz}@pg.gda.pl

The main purpose of this paper is the parameters identification of the Perzyna and the Chaboche models for the aluminum alloy at elevated temperature. The additional purpose is comparison of the results for these viscoplastic models. The results have been verified by the numerical simulation of the laboratory tests. The material parameters have been calculated on the basis of the uniaxial tension test. The determination of the Perzyna model's parameters has been made on the basis of the ideas presented in papers of Perzyna [14–16, 18]. Then the parameters identification of the Chaboche model has been performed using concept presented in [2, 5, 6]. The elastic and inelastic properties have been estimated using the non-linear approximation by the least-squares method in Marquardt-Levenberg variant [12, 13]. The correctness assessment of the performed approximation has been verified by correlation and determination coefficients.

**Key words:** identification, viscoplasticity, Perzyna model, Chaboche model, aluminum, elevated temperature, constant strain-rate tests.

## 1. INTRODUCTION

The viscoplastic constitutive laws defined for small strains can be divided into two groups with respect to the mathematical formulation. The difference between both groups lays in the concept of the creep surface. The first of them, does not use the concept of the creep surface. To this group of models belong: Bodner – Partom, Miller, Krempl, Thanimur, Korhonen, Krieg and Walker models. Therefore, a more complicated mathematical formulation is required to define the transition from the linear elastic range to the inelastic range of deformation. This can be simplified by application of the isotropic internal stress, describing viscoplastic creep surface, which determines the transition between the linear

part and nonlinear part of the strain-stress function. On the other hand it is impossible to take into account the accumulated creep for stresses in the region of the quasi-linear strain-stress function in models. The second group of laws consists of: Perzyna, Chaboche, Aubertin, Lehmann – Imatani and Freed – Virrilli models [9].

The first modern model describing the evolution of viscous effects was proposed by Perzyna in the 1960's [17]. Due to small number of parameters and with relative simple procedure of identification the Perzyna model is still often used for material description in many engineering applications [1]. The extension of the Perzyna law leads to the Chaboche model. The simplest variant of this model is described by seven parameters. The viscoplastic equations of the Chaboche model have been developed and modified many times. The several variants of this model with their practical engineering applications are presented in [2, 5, 22].

## 2. GENERAL FORMULATION OF PERZYNA MODEL AND CHABOCHE MODEL

The viscoplastic constitutive law of Perzyna is based on the condition of perpendicularity of the plastic strain vector increment to the neutral surface (creep surface) in plastic conditions [20]. This is the conclusion of the Drucker postulate. The general formulation of the Perzyna model can be expressed by:

$$(2.1) \quad \dot{E}_{ij}^I = \frac{3}{2} \gamma(T) \langle \Phi(F) \rangle \frac{S'_{ij}}{J(S')}$$

where  $\dot{E}_{ij}^I$  are components of the inelastic strain rate tensor,  $\gamma(T)$  is viscous coefficient dependent on temperature  $\gamma \in (0, \infty)$ ,  $S'_{ij}$  are components of the stress deviator,  $J(S')$  is the second invariant of the stress deviator  $S'_{ij}$ ,  $\Phi(F)$  is optional non-linear function of the viscoplastic potential  $F$ , which can be determined by the formula:

$$(2.2) \quad \Phi(F) = \left\langle \frac{J(S'^{ij})}{R} - 1 \right\rangle^n,$$

or

$$(2.3) \quad \Phi(F) = \left\langle \exp\left(\frac{J(S'^{ij})}{R} - 1\right) - 1 \right\rangle,$$

where  $R$  is temperature dependent hardening parameter (for materials without hardening  $R = k$ ), where  $k$  is initial plasticity limit for zero value of the strain rate,  $n$  is the viscous coefficient. It is possible to meet more complex forms of the function  $\Phi$  [17] used by the Author for high strain rates  $0 \div 10^4 \text{ s}^{-1}$  and assuming  $\gamma = 1$ .

The Chaboche model can be treated as the extension of the Perzyna law. It also assumes existence of the viscoplastic potential [5, 6]. The general formulation of the Chaboche model can be expressed as:

$$(2.4) \quad \dot{E}_{ij}^I = \frac{3}{2} \dot{p} \frac{S'_{ij} - X'_{ij}}{J(S'^{rs} - X'^{rs})},$$

where  $\dot{p}$  is the positive scalar function so-called accumulated inelastic strain rate determined by the formula:

$$(2.5) \quad \dot{p} = \gamma \left\langle \frac{J(S'^{ij} - X'^{ij}) - R - k}{K} \right\rangle^n,$$

where  $K$  is the viscosity parameter,  $X'^{ij}$  are components of the internal stress deviator associated with the kinematic hardening,  $\gamma = 1$  [s<sup>-1</sup>] [9].

### 3. EXPERIMENT DESCRIPTION

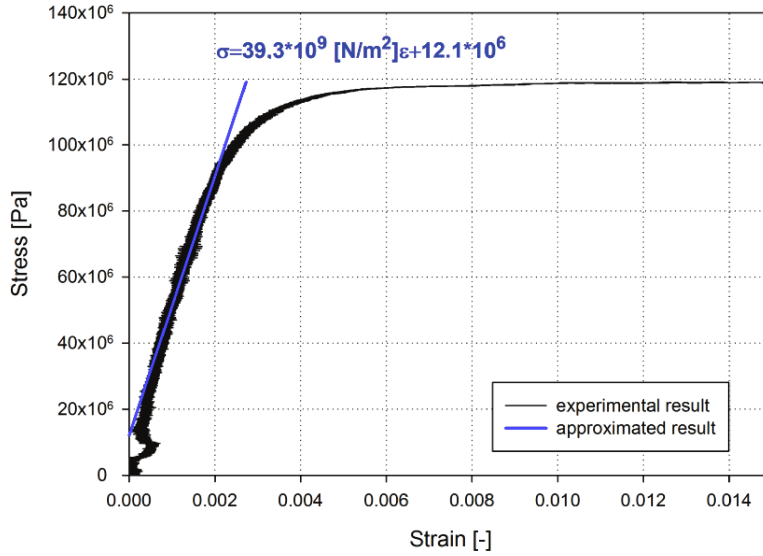
The tests have been performed on the specimens cut out from a 3 mm thick aluminum sheet. The width of each of the specimens is  $b = 24$  mm, while the active length (the distance between the grips of the strength machine)  $l = 70$  mm. The tests have been performed on a strength machine Zwick/Roell Z400 with the mechanical extensometer (active length  $l_0 = 30$  mm) and a thermal chamber. Due to the fact that viscoplastic phenomena in metals manifests particularly at elevated temperature it has been decided that the tests would be carried out at temperature of 120°C. The experiments have been conducted for five strain rates:  $10^{-4}$ ,  $5 \cdot 10^{-4}$ ,  $10^{-3}$ ,  $5 \cdot 10^{-3}$ ,  $10^{-2}$  s<sup>-1</sup>. For each strain rate at least three tests have been performed. In each tests about 2000 sets of time, displacement and force values have been recorded using a computer.

### 4. IDENTIFICATION OF PARAMETERS

#### 4.1. Identification of the elastic properties

The linear range for each test has been estimated on the basis of the stress-strain graphs. Next, the elasticity modulus  $E$  has been calculated. Generally, the stress-strain function for the tested specimens is linear for the strain range of between about 0.0005 to 0.002. This strain range corresponds to the stress range of approximately from 30 to 90 MPa (Fig. 1).

The value Young's modulus  $E$  in each test has been determined by performing a linear approximation in the range specified above. The final values of the elasticity modulus obtained at elevated temperature (120°C) are shown in Table 1.

FIG. 1. Identification of an elasticity modulus  $E$ .**Table 1.** The values of the Young's modulus.

Reference strain rate [s <sup>-1</sup> ]	Values of Young's modulus [GPa]	Average values of Young's modulus [GPa]	Values of standard deviation $\sigma_y$ [GPa]	Values of coefficient of variation $s$ [%]
10 <sup>-4</sup>	35.5	38.1	1.840	4.8
	39.3			
	39.5			
5·10 <sup>-4</sup>	38.8	41.2	3.394	8.2
	46.0			
	38.8			
10 <sup>-3</sup>	41.3	44.1	2.774	6.3
	47.9			
	43.2			
5·10 <sup>-3</sup>	56.1	56.5	2.428	4.3
	59.7			
	53.8			
10 <sup>-2</sup>	62.9	57.5	3.955	6.9
	53.6			
	55.9			

While analyzing this table, it has been noted that at temperature of 120°C the values of the elasticity modulus increase with the strain rate increase. This is why the average value of the Young's modulus has been calculated for each strain rate separately.

#### 4.2. Identification of inelastic parameters

4.2.1. *The identification process of Perzyna model.* The parameters identification should begin with the determination of the initial plasticity limit at zero strain rate, what gives the value of the parameter  $k$ . For this purpose the stress-strain rate graph has been created, and stress value at the plasticity limit for each of five strain rates has been determined. For this purpose the criterion of the plasticity limit is chosen according to [19]. It is the value of stress when difference between the experimental curve and the elastic function obtained in the Young's modulus identification is bigger than 0.2% (Fig. 2). It can be also interpreted as the value of stress when the inelastic strain is equal to  $\varepsilon_p = 0.2\%$ .

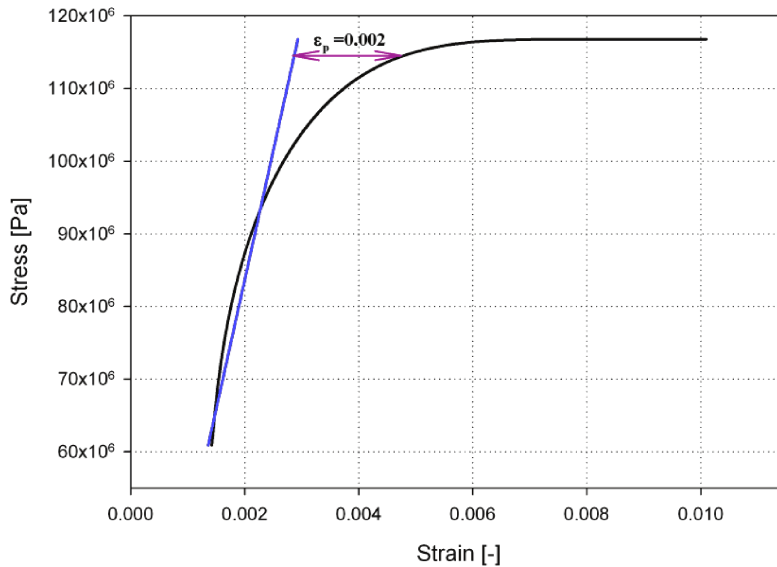


FIG. 2. Calculating the plasticity limit on the basis of the stress-strain graph.

It has been assumed that in the initial phase of inelastic deformation the inelastic strain rate is almost equal to the total strain rate  $\dot{\varepsilon}_p \approx \dot{\varepsilon}$ . Therefore in this paper, when determining parameters, the values of the inelastic strain rate  $\dot{\varepsilon}_p$  have been replaced with the values of the total strain rate  $\dot{\varepsilon}$  in all equations. At the same time, the values of the strain rate have been calculated on the basis of the experimental results to validate the settings of the strength machine. It has been assumed that the tests have been made at a constant strain rate. The time-strain graphs have been made in order to confirm the validity of the assumption. In the tests (especially with higher strain rates) it has been difficult to reach assumed strain rate already in the elastic range of deformation. Consequently during tests the elasticity limit has been achieved with the values of the strain

rate different than it was assumed before the test. Thus, calculating  $k$  parameter, the real strain rate corresponding to the plasticity limit has been used. The obtained results of the strain rate and of the plasticity limit for all the tests are presented in Table 2.

**Table 2.** The values of the plasticity limit and strain rate.

Reference strain rate [s <sup>-1</sup> ]	Values of plasticity limit [MPa]	Average values of the plasticity limit [MPa]	Actual value of strain rate [s <sup>-1</sup> ]	Average values of strain rate [s <sup>-1</sup> ]
10 <sup>-4</sup>	114.850	114.909	1.078·10 <sup>-4</sup>	1.606·10 <sup>-4</sup>
	116.300		1.838·10 <sup>-4</sup>	
	113.578		1.901·10 <sup>-4</sup>	
5·10 <sup>-4</sup>	114.185	115.523	8.830·10 <sup>-4</sup>	9.406·10 <sup>-4</sup>
	116.771		8.668·10 <sup>-4</sup>	
	115.612		1.072·10 <sup>-3</sup>	
10 <sup>-3</sup>	116.505	116.854	1.864·10 <sup>-3</sup>	1.610·10 <sup>-3</sup>
	118.207		1.511·10 <sup>-3</sup>	
	115.850		1.454·10 <sup>-3</sup>	
5·10 <sup>-3</sup>	118.451	117.395	5.666·10 <sup>-3</sup>	6.724·10 <sup>-3</sup>
	117.715		6.346·10 <sup>-3</sup>	
	116.018		8.161·10 <sup>-3</sup>	
10 <sup>-2</sup>	118.013	117.747	1.452·10 <sup>-2</sup>	1.259·10 <sup>-2</sup>
	116.819		1.226·10 <sup>-2</sup>	
	118.409		1.100·10 <sup>-2</sup>	

Next, the stress-strain rate graph has been made due to calculated average values of the elastic limit and the average values of the strain rate shown in Table 2. This function has been approximated with the formula:

$$(4.1) \quad \sigma = y_0 + a(1 - \exp(-b\dot{\epsilon}_p)) + c(1 - \exp(-d\dot{\epsilon}_p)),$$

where  $y_0$ ,  $a$ ,  $b$ ,  $c$ ,  $d$  are requested coefficient of this equation. This graph with the approximated function has been shown in Fig 3.

According to this graph the value of parameter  $k = 114$  [MPa]. This value has been used for estimation of two other parameters  $\gamma$  and  $n$ . For the same stress-strain rate graph has been determined other parameters of the Perzyna model have been obtained from the equation in uniaxial variant using the non-linear regression:

$$(4.2) \quad \dot{\epsilon}_p = \gamma \left( \frac{\sigma}{k} - 1 \right)^n.$$

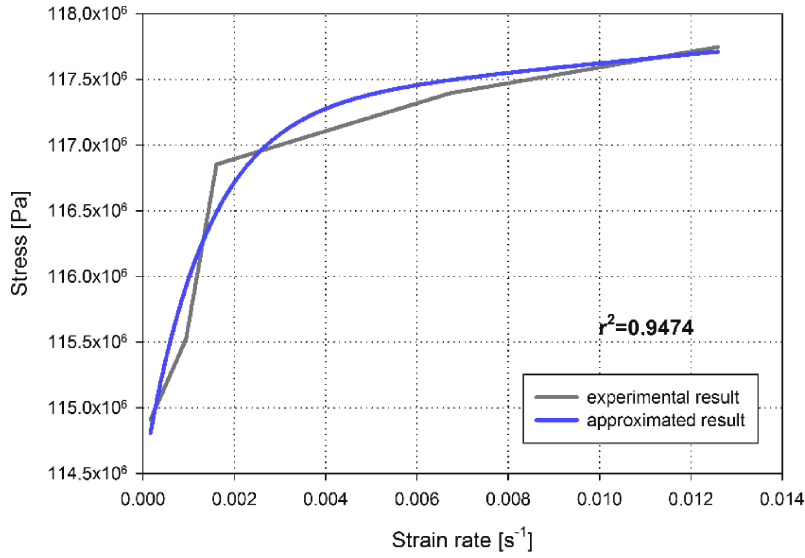


FIG. 3. Stress-strain rate graph with the approximated function – parameter  $k$  determination.

The parameter  $k$  has been estimated separately, because its value is also necessary for the Chaboche model parameters' identification. The stress-strain rate graph for the obtained values of  $\gamma$  and  $n$  parameters and the experimental curve are shown in Fig. 4.

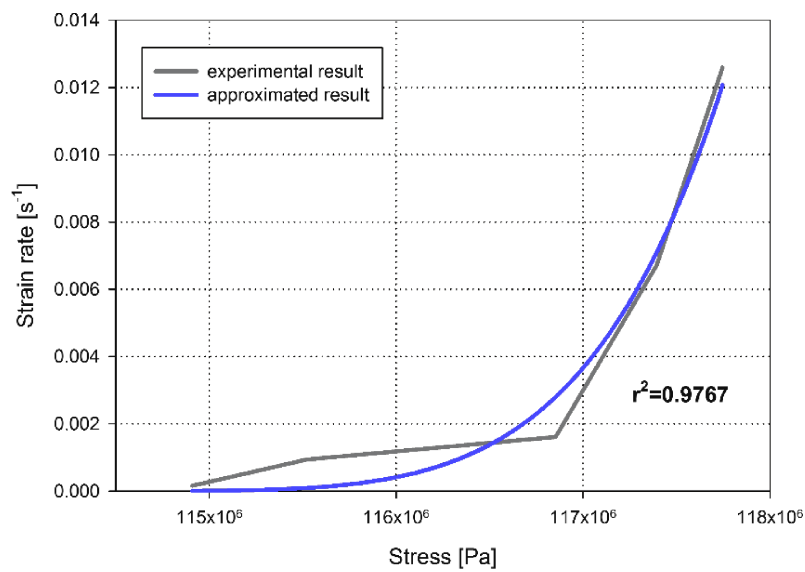


FIG. 4. Stress-strain rate graph with approximated function.

The obtained values of parameters of the Perzyna model are presented in Table 3.

**Table 3.** Parameters of Perzyna's model.

Parameter	Unit	Values of the parameters
$k$	MPa	114.0
$n$	–	5.37
$\gamma$	$s^{-1}$	$1.10 \cdot 10^6$

*4.2.2. The identification process of Chaboche model.* In case of the Chaboche model the best way of parameters identification is using the results of the cyclic tests [11]. But this tests cannot be performed for many kinds of materials and shapes of specimens, due to the buckling effect or properties of the material (e.g. for textile fabrics, soft composites). In this paper identification on the basis of uniaxial tension tests is presented. Such regression is rather difficult, because it is necessary to identify from non-linear equations all parameters at the same time. It is not possible to separate hardenings functions from viscous effects. The basis variant of the Chaboche model have the following seven number of parameters:  $k, K, n, a, c, b, R_1$ . The first parameter  $k$  has been estimated in the previous chapter. The other six parameters have to be calculated on the basis of the equation for the uniaxial load case. Such set of equations can be obtained from relations given in Chapter 2.

$$(4.3) \quad \begin{aligned} \dot{p} = |\dot{\epsilon}_p| &= \gamma \left\langle \frac{|\sigma - X| - R - k}{K} \right\rangle^n, \\ \dot{\epsilon}_p &= \gamma \left\langle \frac{|\sigma - X| - R - k}{K} \right\rangle^n \operatorname{sgn}(\sigma - X), \end{aligned}$$

$$(4.4) \quad \begin{aligned} \dot{X} &= \frac{2}{3} a \dot{\epsilon}_p - c X |\dot{\epsilon}_p|, \\ \dot{R} &= b(R_1 - R) |\dot{\epsilon}_p|, \end{aligned}$$

where  $a$  is the saturation value of internal stress  $X^{ij}$  in the uniaxial case,  $c$  is parameter, which controls the convergence velocity of a model to stabilized cycle,  $b$  is the coefficient, which influences the convergence rate of a model to stabilized cycle,  $R_1$  is parameter, which is responsible for the cyclic fatigue effects ( $R_1 < 0$ ) or cyclic strengthening effects ( $R_1 > 0$ ), what means that increases or decreases



the amplitude of plastic strain in each cycles. Both hardening functions in the uniaxial stress state can be integrated explicitly:

$$(4.5) \quad \begin{aligned} X &= \nu \frac{2a}{3c} + \left( X_0 - \frac{2a}{3c} \right) \exp(-c(\varepsilon_p - \varepsilon_{p0})), \\ R &= R_1 (1 - \exp(-b|\varepsilon_p|)), \end{aligned}$$

where  $X$  is kinematic hardening,  $X_0$  is initial kinematic hardening,  $\varepsilon_p$  is inelastic strain,  $\varepsilon_{p0}$  is initial inelastic strain,  $\nu = \text{sgn}(\sigma - X) = \pm 1$  for uniaxial tension test  $\nu = 1$ ,  $R$  is isotropic hardening. The final formula for stresses useful for the identification of parameters has the form:

$$(4.6) \quad \sigma = X(\varepsilon_p, X_0, \varepsilon_{p0}) + \nu R(|\varepsilon_p|) + \nu k + \nu K |\dot{\varepsilon}_p|^{1/n},$$

where  $\dot{\varepsilon}_p$  is inelastic strain rate. For uniaxial tension tests proceed  $X_0 = 0$  and  $\varepsilon_{p0} = 0$ , therefore the hardening functions can be expressed as:

$$(4.7) \quad \begin{aligned} X &= \frac{2a}{3c} [1 - \exp(-c\varepsilon_p)], \\ R &= R_1 [1 - \exp(-b\varepsilon_p)]. \end{aligned}$$

For the identification process one representative test for each strain rate has been selected. First, the stress-time and strain-time functions have been approximated using the least – squares method. It has been made as the differentiation of these functions is necessary. The stress-time functions have been approximated by the four-parameters Weibull's functions. Then the strain-time functions have been determined by the polynomial functions. According to the character of the certain test the fifth – degree, fourth – degree or third – degree polynomial functions have been applied. For the lower strain rate test higher order of the polynomial function has been used. Next by the numerical differentiation (central differences method) the strain rate function has been found. In order to estimate the parameters of the Chaboche model, it has been collected data of stress, strain and strain rate for selected tests. Then such collected function has been approximated using the Eqs. (4.6) and (4.7). The parameters identification has been performed by the Marquardt-Levenberg algorithm [12, 13]. The results are shown in Fig. 5. The presented regression method requires the initial values of the desired parameters. In case of the Chaboche model, identification results often depend on the initial values of parameters, so can be ambiguous. In this paper, the initial values of parameters have been assumed from the literature [9]. The values of parameters identification of the Chaboche model have been presented in Table 4.

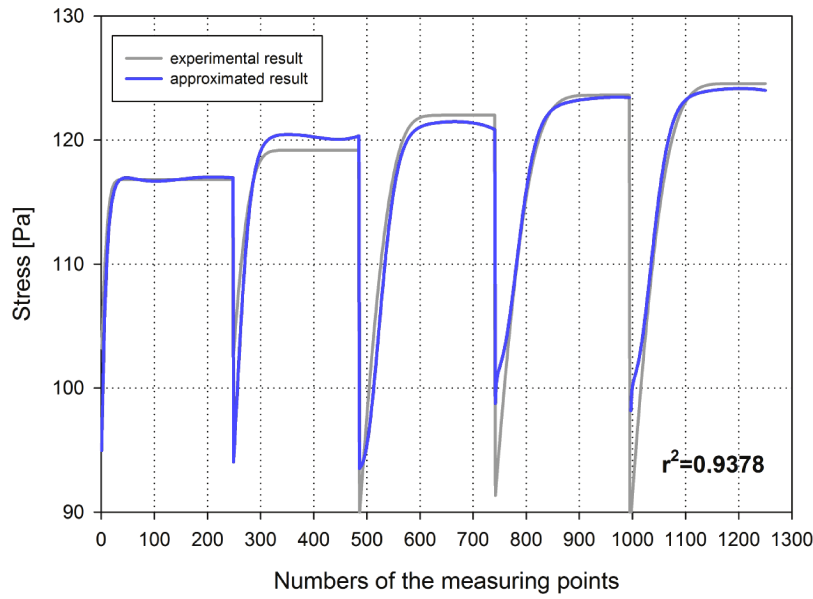


FIG. 5. Number of measuring points – stress graph with approximated function.

**Table 4.** Parameters of Chaboche model.

Parameter	Unit	Values of the parameters
$k$	MPa	114.0
$K$	MPa	-11.69
$n$	-	-13.66
$a$	MPa	$3.429 \cdot 10^4$
$c$	-	905
$b$	-	15.84
$R_1$	MPa	3.262

The values of the correlation and determination coefficients are close or equal to 1.0, what indicates good quality of the performed approximation. The additional formulas on the basis of which the accuracy of the approximation has been evaluated, can be found in the works [7] and [21].

## 5. VERIFICATION OF APPROXIMATION RESULTS

The next important step determining the inaccuracy of the identification assessing is the verification of obtained results by the numerical simulation of experiments. The algorithm which has been used for the verification relates to

the system with one degree of freedom and allows to simulate the static tensile tests made in different conditions. The details of the algorithm implemented in the program are given in [9]. The results of the verification for the Perzyna and Chaboche models' parameters have been compared with the experimental results by the stress-strain function. In order to assess the accuracy of the per-

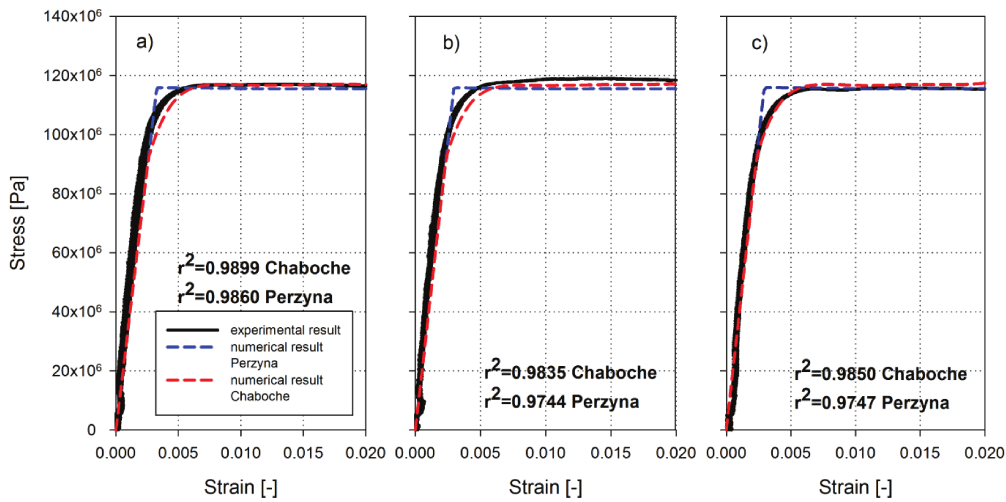


FIG. 6. The results of the numerical simulation of the tension tests of the aluminum alloy at the strain rate of  $10^{-4}$  [s<sup>-1</sup>] compared with the results for each specimen (a, b, c).

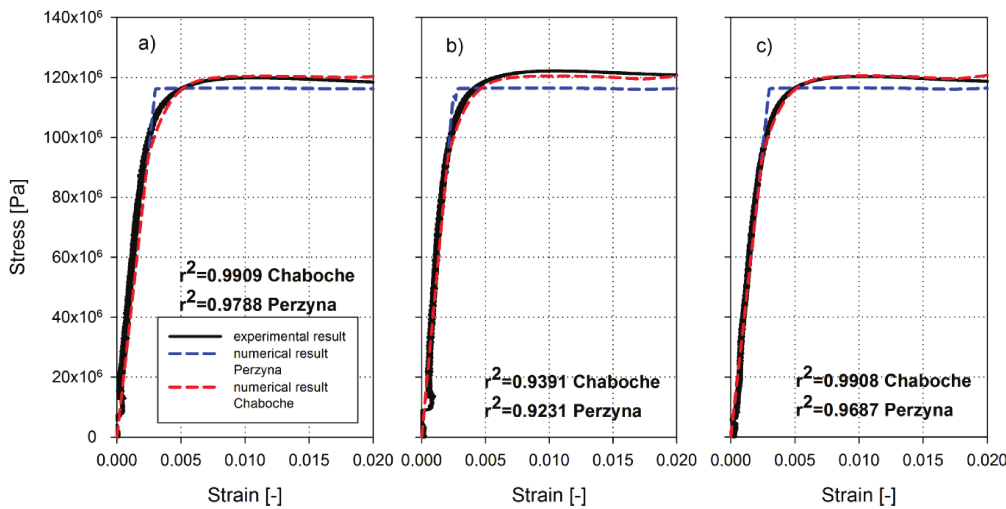


FIG. 7. The results of the numerical simulation of the tension tests of the aluminum alloy at the strain rate of  $5 \cdot 10^{-4}$  [s<sup>-1</sup>] compared with the results for each specimen (a, b, c).

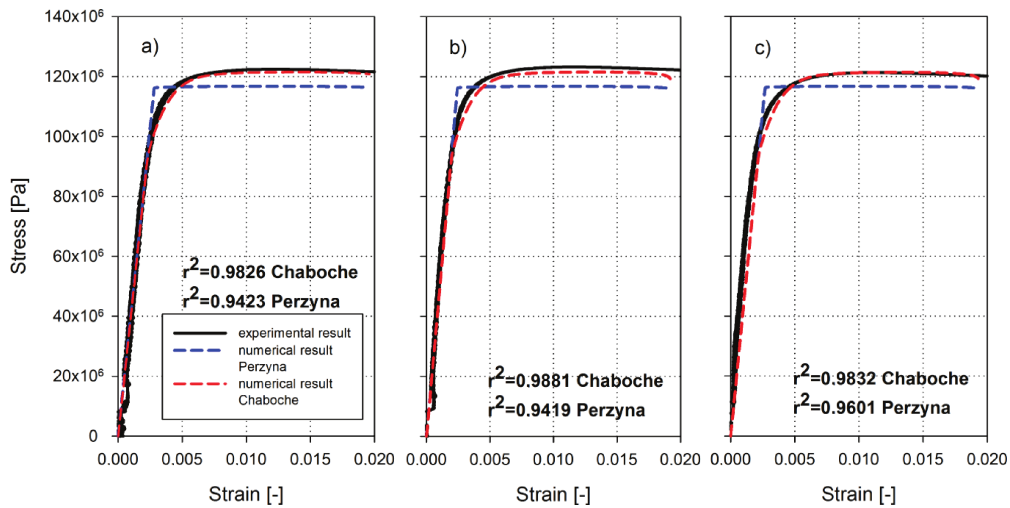


FIG. 8. The results of the numerical simulation of the tension tests of the aluminum alloy at the strain rate of  $10^{-3}$  [s $^{-1}$ ] compared with the results for each specimen (a, b, c).

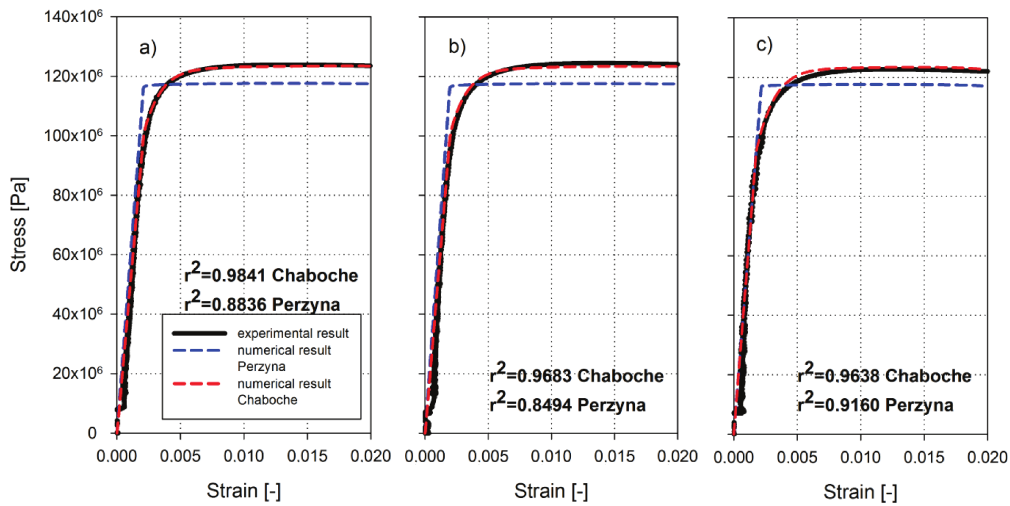


FIG. 9. The results of the numerical simulation of the tension tests of the aluminum alloy at the strain rate of  $5 \cdot 10^{-3}$  [s $^{-1}$ ] compared with the results for each specimen (a, b, c).

formed verification with the experimental data the determination coefficients  $r^2$  have been calculated. Figures 6–10 present the comparison of the results of the performed numerical simulation with the experimental results for selected tests. Calculations confirm good quality of the identification results.

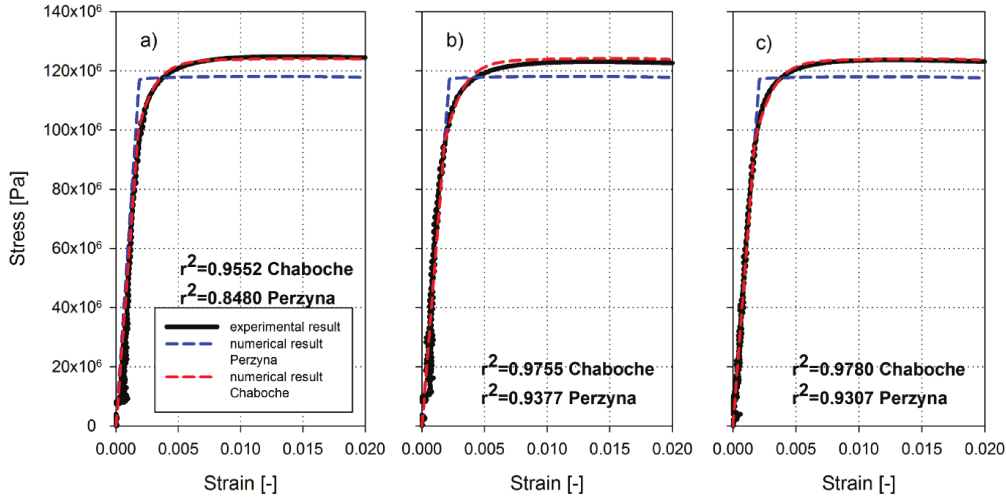


FIG. 10. The results of the numerical simulation of the tension tests of the aluminum alloy at the strain rate of  $10^{-2}$  [s $^{-1}$ ] compared with the results for each specimen (a, b, c).

## 6. CONCLUSIONS

In the paper examples of successful identification of viscoplastic constitutive models for aluminum alloy has been performed. Two viscoplastic models, having the same origin have been considered. The older one (Perzyna model) in the presented historical form has the isotropic hardening (in the implicit form) and no kinematic hardening function and is restricted to three inelastic parameters. The Chaboche model, which is extension of the Perzyna model in fact has explicit kinematic and isotropic hardening functions. On the other hand it is necessary to identify at least 7 material parameters. The best way to receive them is to make fully reversed cyclic test, but this type of tests for large group of materials and structures is not possible. Identification from tensile tests with different strain rates is also possible, but is much more difficult what also means that is less accurate.

The performed verification of the tests show that both investigated constitutive model can express behavior of the investigated aluminum alloy in elevated temperature. The authors confirmed once more that a simpler constitutive laws (like Perzyna model) can express quite well material behavior. The similar conclusion can be found in [3, 4] and [8], where the example of explosion on aluminum shell is investigated.

In the current research the dependence of the Young's modulus on the strain rate at elevated temperature is observed.

Obtained conclusions will be confirmed in the near future by following experiments and calculations of structures.

## REFERENCES

1. AMBROZIAK A., KŁOSOWSKI P., NOWICKI M., SCHMIDT R., *Implementation of continuum damage in elasto-viscoplastic constitutive equations*, Task Quarterly, **10**, 2, 207–220, 2006.
2. AMBROZIAK A., KŁOSOWSKI P., *The elasto-viscoplastic Chaboche model*, Task Quarterly **10**, 1, 49–61, 2006.
3. ARGYRIS J., BALMER H.A., DOLTSINIS I.St., *On Shell Models for Impact Analysis*, The Winter Annual Meeting of the American Society of Mechanical Engineers, **3**, 443–456, 1989.
4. BELYTSCHKO T., WONG B.L., CHIANG H.Y., *Improvements in Low-Order Shell Elements for Explicit Transient Analysis*, The Winter Annual Meeting of the American Society of Mechanical Engineers, **3**, 383–398, 1989.
5. CHABOCHE J.L., *Constitutive equations for cyclic plasticity and cyclic viscoplasticity*, Int. J. Plasticity, **5**, 247–302, 1989.
6. CHABOCHE J.L., *Viscoplastic constitutive equations for the description of cyclic and anisotropic behavior of metals*, 17th Polish Conf. on Mechanics of Solid, Szczyrk, Bul. De l'Acad. Polonaise des Sciences, Serie Sc. Et Techn., **25**, 33–42, 1977.
7. CHAPRA S.C., CANALE R.P., *Numerical Methods for Engineers*, McGraw-Hill Book Company, New York, 1988.
8. KŁOSOWSKI P., *Nonlinear numerical analysis and experimental tests of vibrations of elastic-viscoplastic plates and shells* [in Polish], Monographs, Ed. Gdańsk University of Technology, Gdańsk, 1999.
9. KŁOSOWSKI P., WOZNICA K., *Nonlinear viscoplastic constitutive models in selected applications of structures analysis* [in Polish], Ed. Gdańsk University of Technology, Gdańsk, 2007.
10. KŁOSOWSKI P., ZAGUBIEŃ A., WOZNICA K., *Investigation on rheological properties of technical fabric "Panama"*, Arch. Appl. Mech., **73**, 661–681, 2004.
11. LEMAITRE J., CHABOCHE J.L., *Mechanics of Solid Materials*, Cambridge University Press, Cambridge, 1990.
12. LEVENBERG K., *A method for the solution of certain problems in least squares*, Quart. Appl. Math., **2**, 164–168, 1944.
13. MARQUARDT D.W., *An Algorithm for Least Squares Estimation of Parameters*, Journal of the Society of Industrial and Applied Mathematics, **11**, 431–441, 1963.
14. PERZYNA P., *Fundamental problems in viscoplasticity*, Advances in Mechanics, **9**, 243–377, 1966.
15. PERZYNA P., *On the constitutive equations for work-hardening and rate sensitive plastic materials*, Proc. Vibr. Probl., **4**, 281–290, 1963.
16. PERZYNA P., *The constitutive equations for rate sensitive plastic materials*, Quart. Appl. Mech., **20**, 321–32, 1963.
17. PERZYNA P., *The study of the dynamic behavior of rate sensitive plastic materials*, Archives of Mechanics, **1**, 15, 113–129, 1963.
18. PERZYNA P., *Theory of viscoplasticity* [in Polish], PWN, Warsaw, 1966.

19. ROWLEY M.A., THORNTON E.A., *Constitutive Modeling of the Visco-Plastic Response of Hastelloy – X and Aluminium Alloy 8009*, Jour. of Engng. Materials and Technology, **118**, 19–27, 1996.
20. SKRZYPEK J., *Plasticity and creep* [in Polish], PWN, Warsaw, 1986.
21. TAYLOR J.R., *Introduction to error analysis*, PWN, Warsaw, 1995.
22. WOZNICA K., *Dynamique des structures elasto-viscoplastiques*, Cahiers de Mécanique, Lille, 1998.

*Received May 29, 2014; revised version November 2, 2014.*

---